Potential Poroelastic Triggering of the 2020 M5.0 Mentone Earthquake in the Delaware Basin, Texas, by Shallow Injection Wells

Supplemental Material

by Xinyu Tan and Semechah K. Y. Lui

Contents of this file

Figures S1 to S15

Tables S1 to S10

Video S1

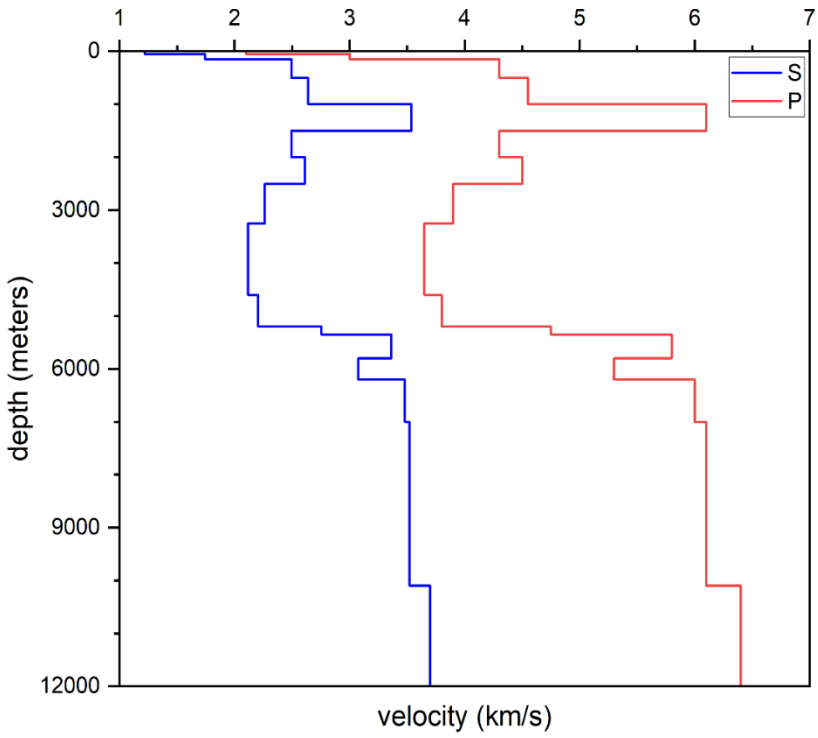

Figure S1. Velocity model used in CAP inversion (modified from Sheng et al., 2022).

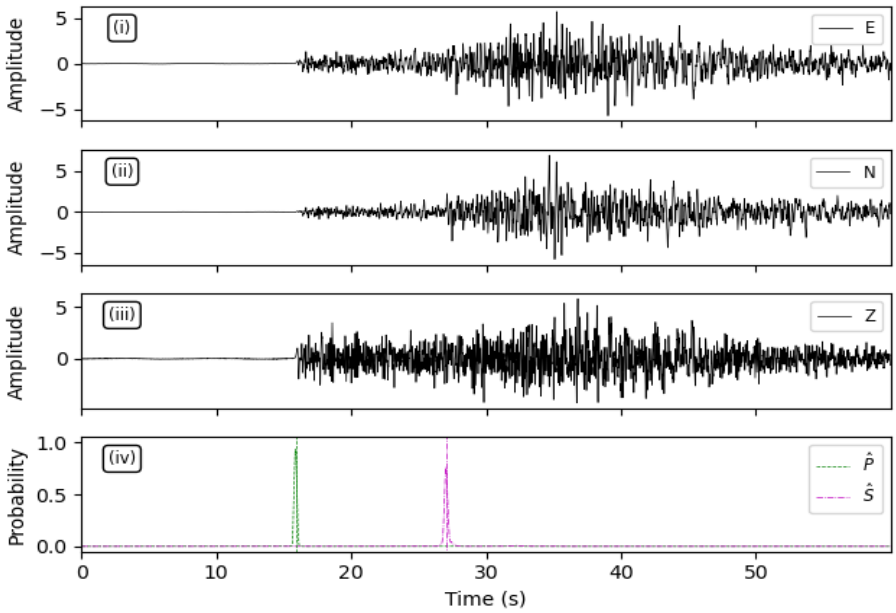

Figure S2. Example of phase pick output from PhaseNet.

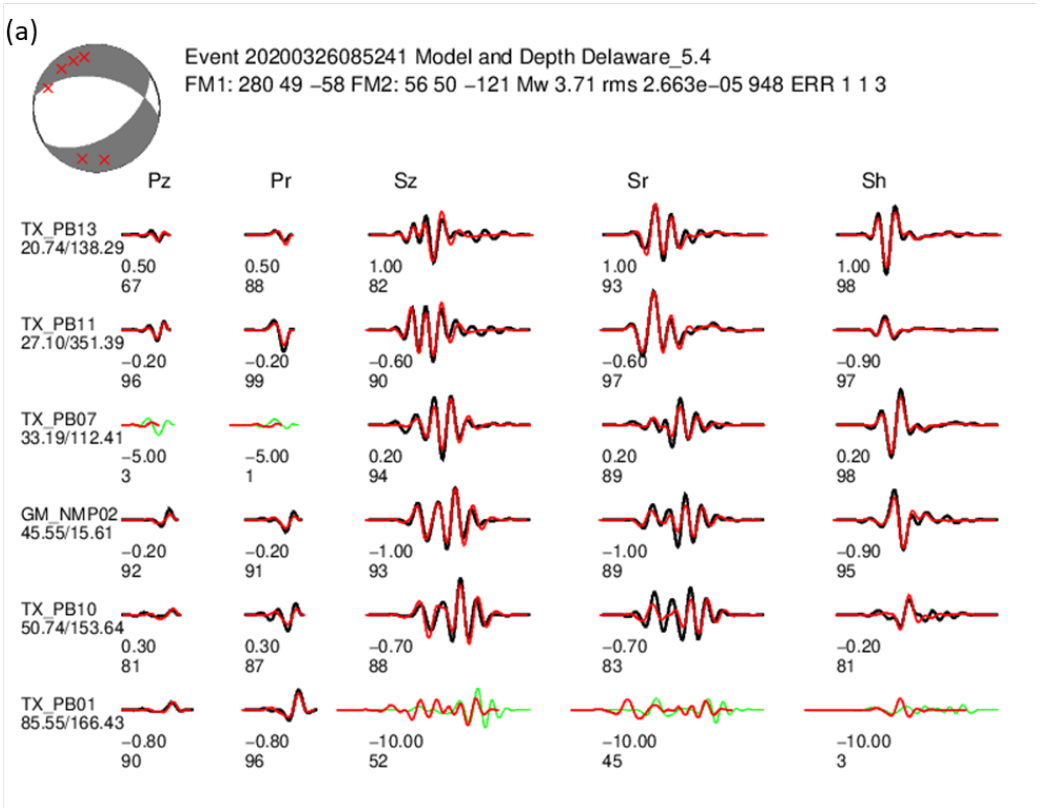

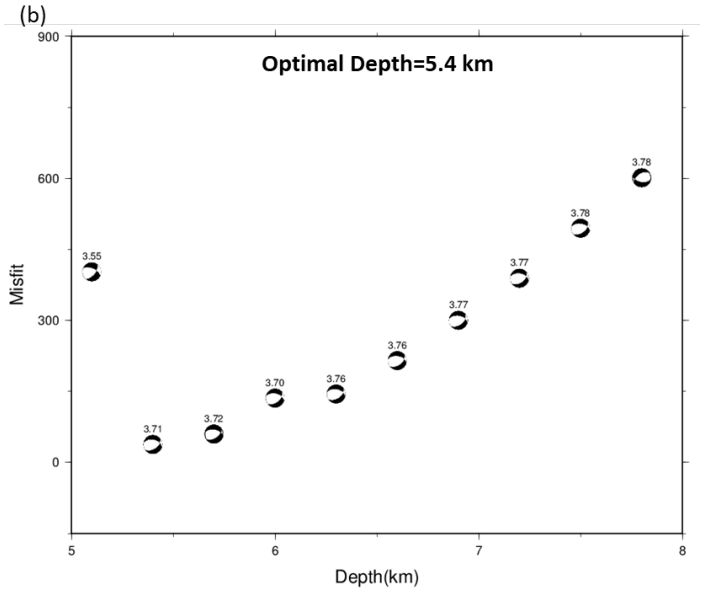

Figure S3. (a) Cross correlation (cc) of synthetic (red) and actual (black) waveforms at the optimal depth of event 02. Green waveforms are below the cc threshold and not accounted for in inversion results. The numbers below the waveforms are optimal shift time (in second) and cross correlation, respectively. (b) Relative misfit error of event 02 inversion at different focal depths.

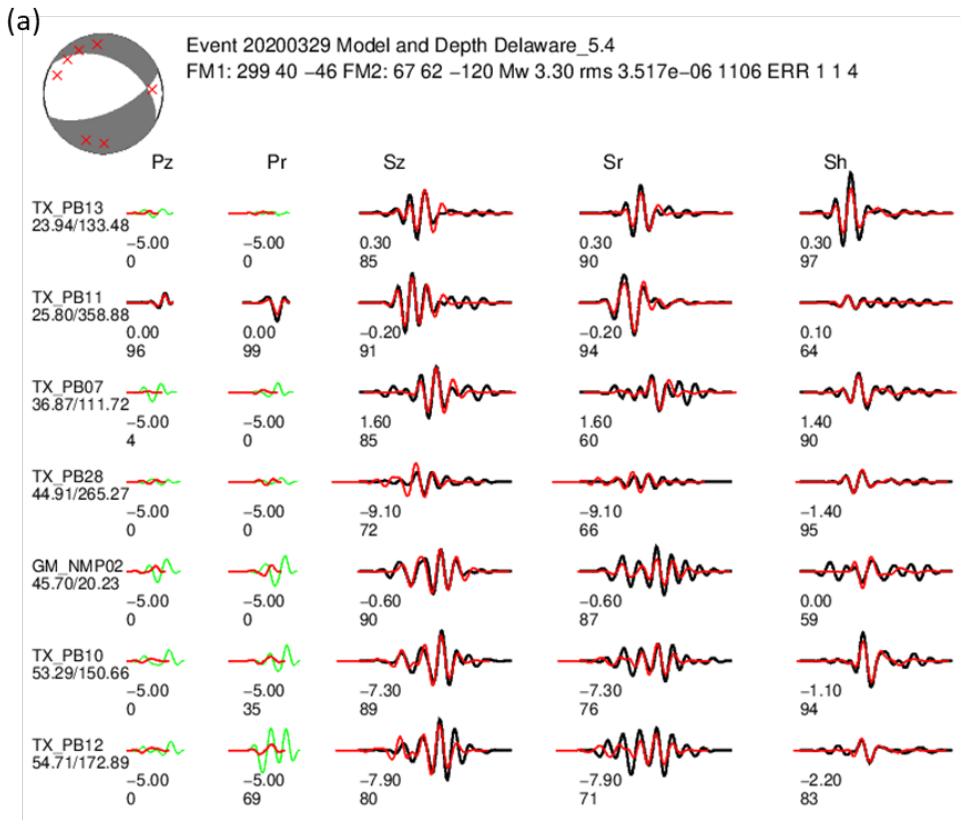

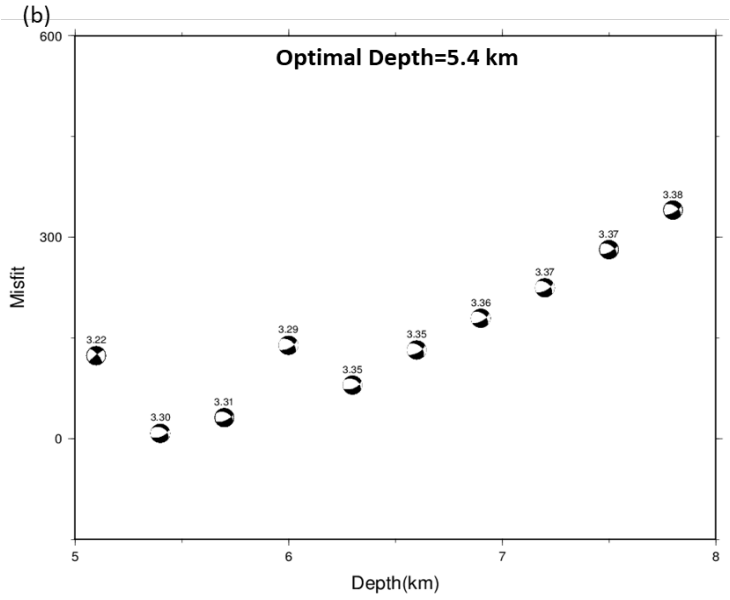

Figure S4. (a) Cross correlation (cc) of synthetic (red) and actual (black) waveforms at the optimal depth of event 03. Green waveforms are below the cc threshold and not accounted for in inversion results. The numbers below the waveforms are optimal shift time (in second) and cross correlation, respectively. (b) Relative misfit error of event 03 inversion at different focal depths.

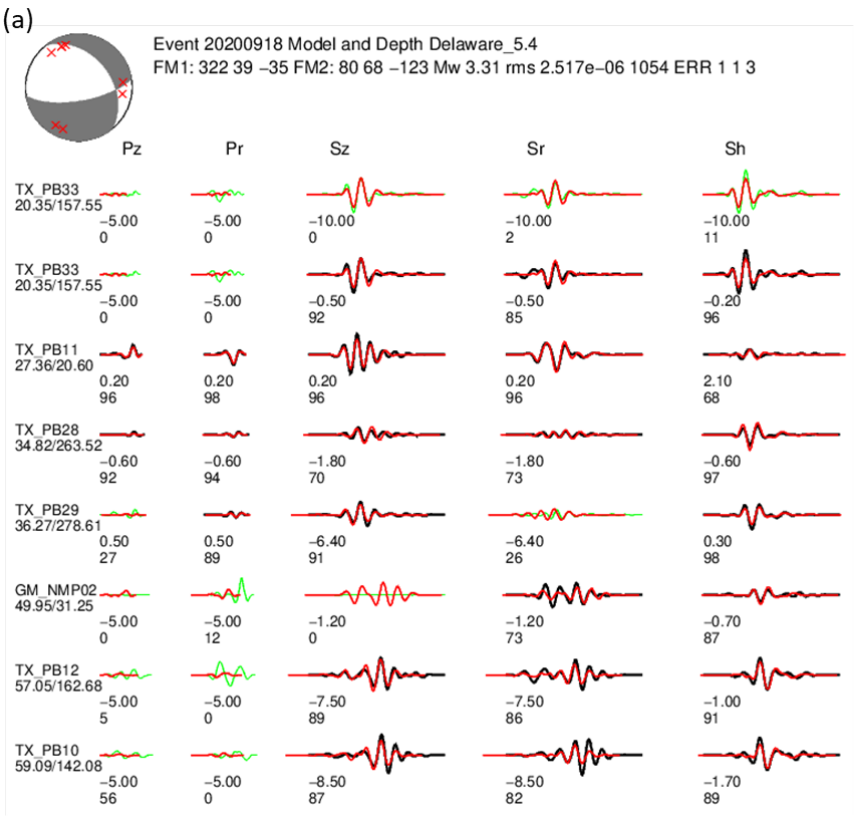

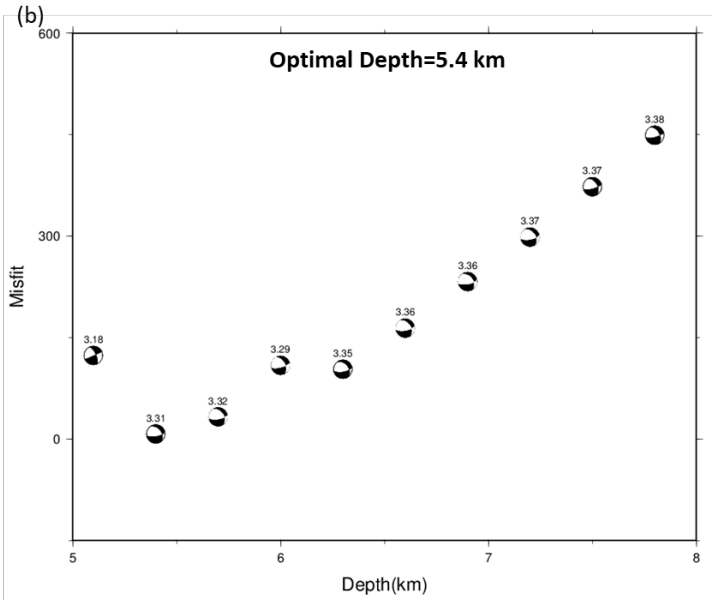

Figure S5. (a) Cross correlation (cc) of synthetic (red) and actual (black) waveforms at the optimal depth of event 04. Green waveforms are below the cc threshold and not accounted for in inversion results. The numbers below the waveforms are optimal shift time (in second) and cross correlation, respectively. (b) Relative misfit error of event 04 inversion at different focal depths.

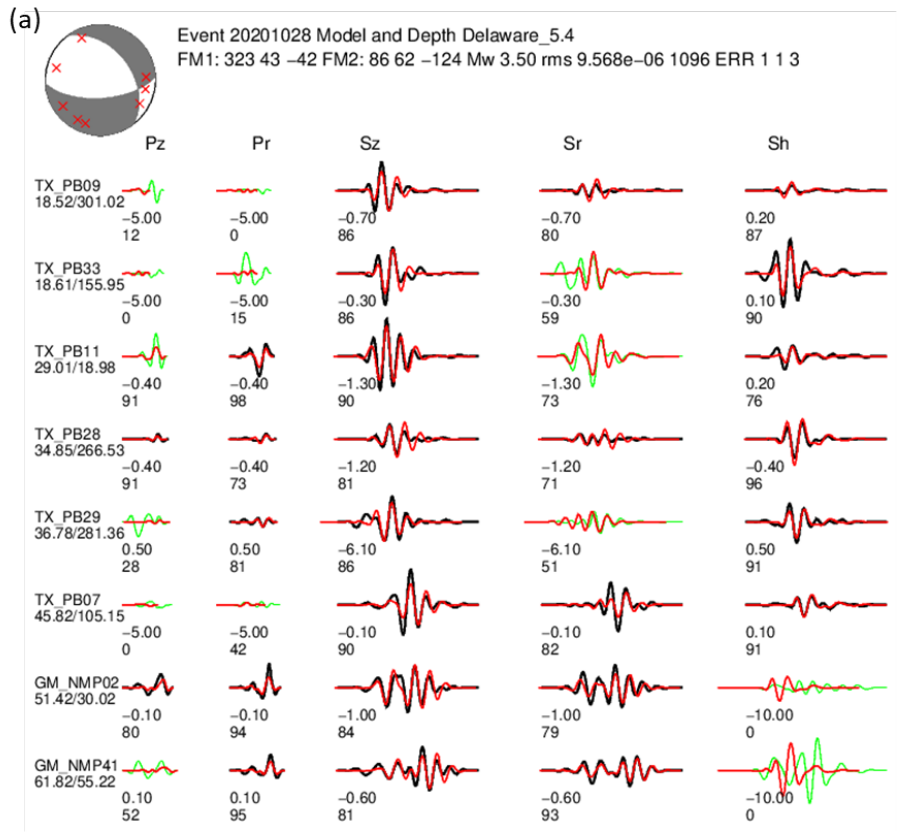

37

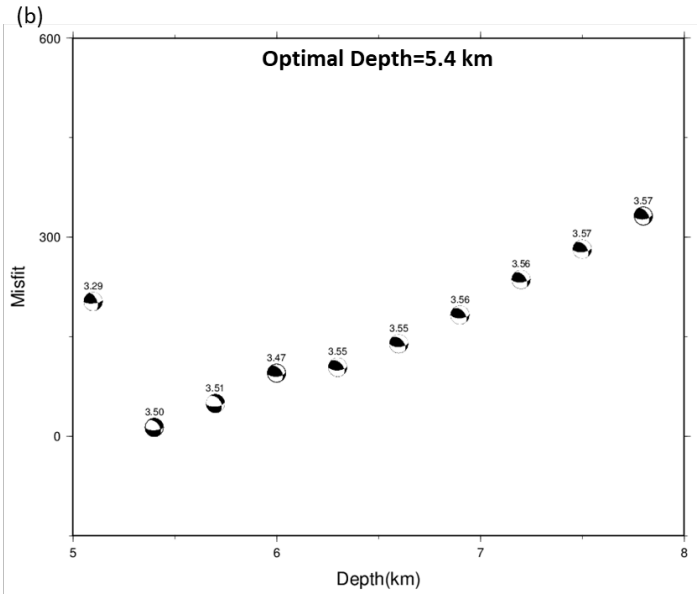

38

39 **Figure S6.** (a) Cross correlation (cc) of synthetic (red) and actual (black) waveforms at the
40 optimal depth of event 05. Green waveforms are below the cc threshold and not accounted for in
41 inversion results. The numbers below the waveforms are optimal shift time (in second) and cross
42 correlation, respectively. (b) Relative misfit error of event 05 inversion at different focal depths.

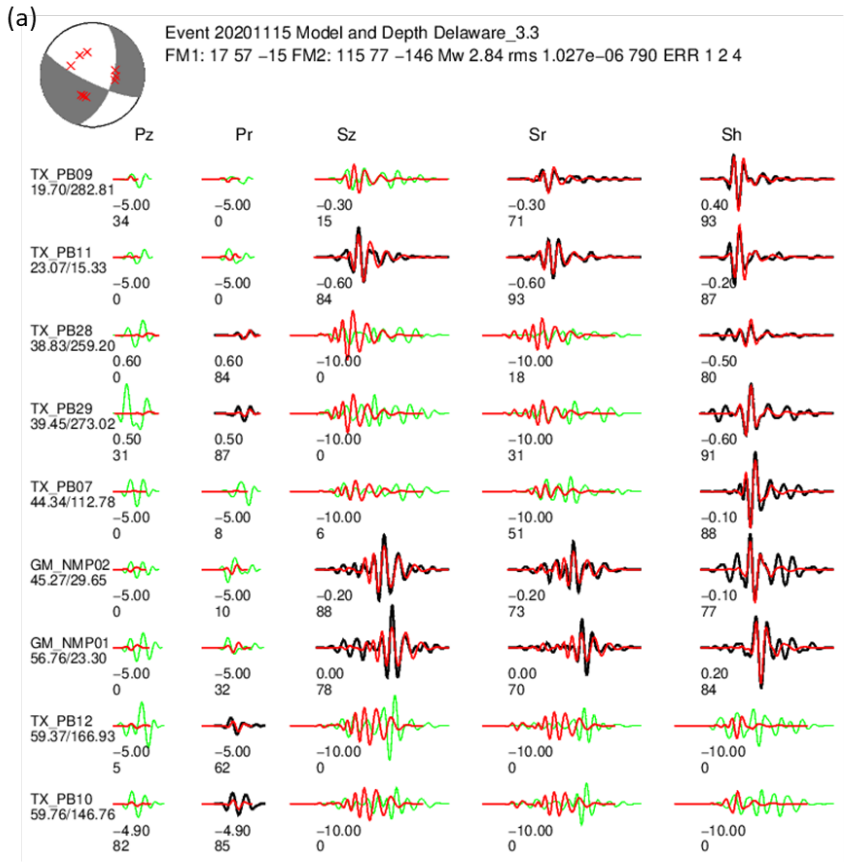

43

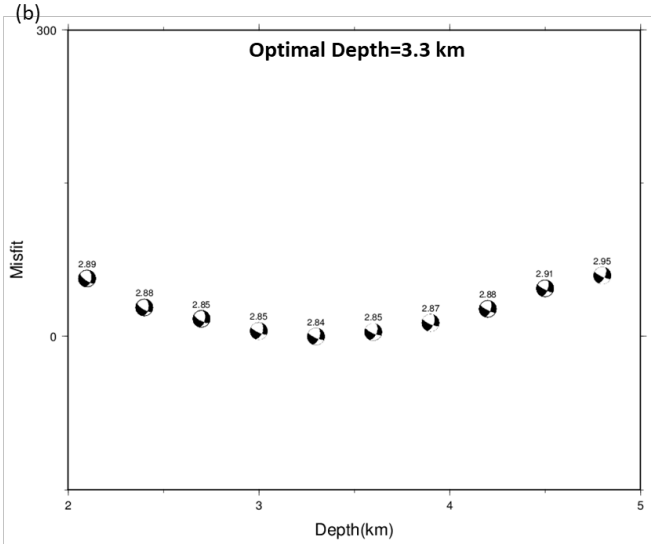

44

45 **Figure S7.** (a) Cross correlation (cc) of synthetic (red) and actual (black) waveforms at the
46 optimal depth of event 06. Green waveforms are below the cc threshold and not accounted for in
47 inversion results. The numbers below the waveforms are optimal shift time (in second) and cross
48 correlation, respectively. (b) Relative misfit error of event 06 inversion at different focal depths.

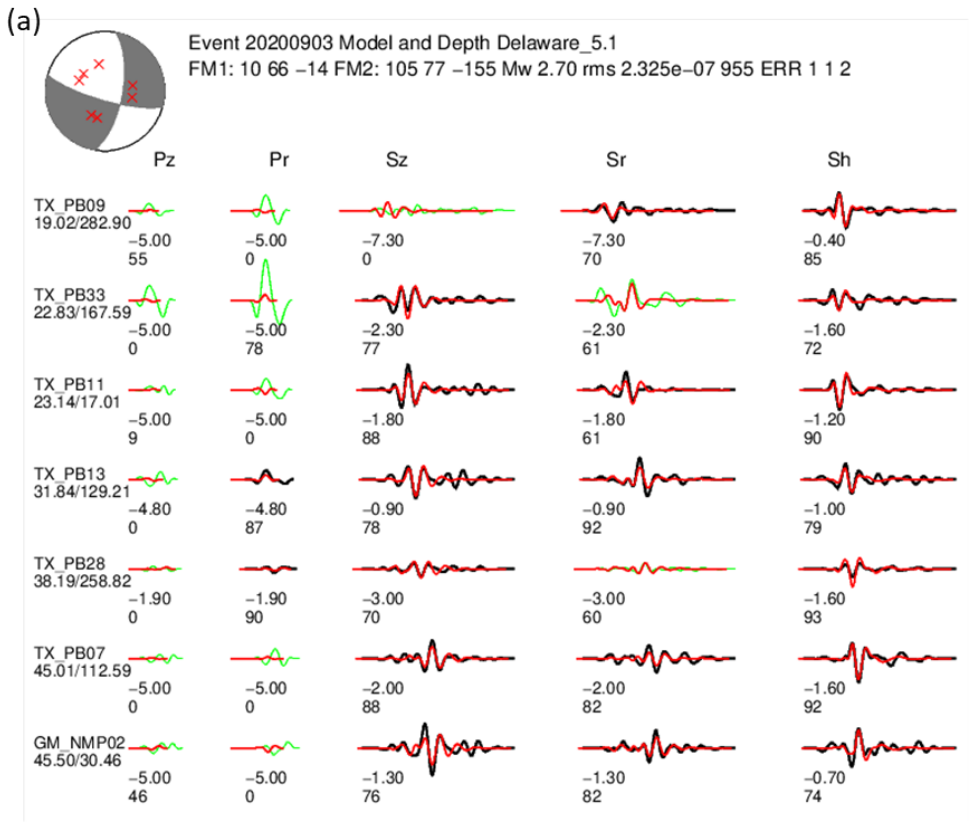

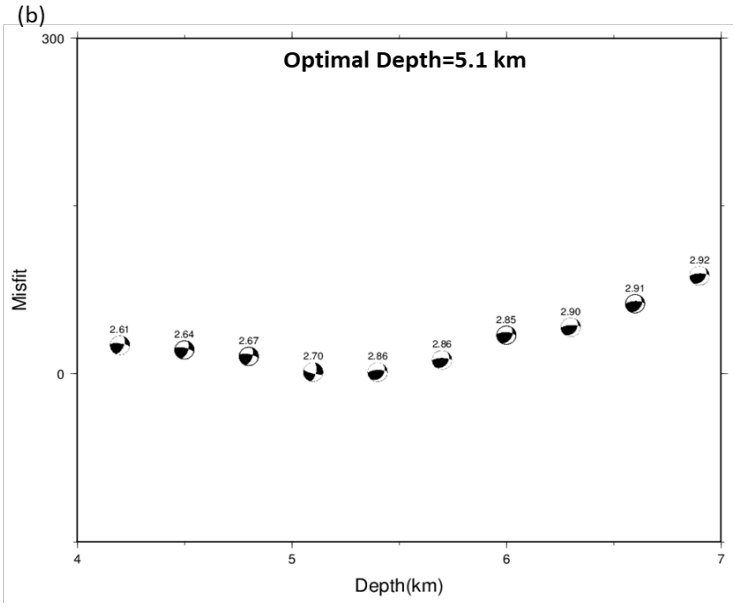

Figure S8. (a) Cross correlation (cc) of synthetic (red) and actual (black) waveforms at the optimal depth of event 07. Green waveforms are below the cc threshold and not accounted for in inversion results. The numbers below the waveforms are optimal shift time (in second) and cross correlation, respectively. (b) Relative misfit error of event 07 inversion at different focal depths.

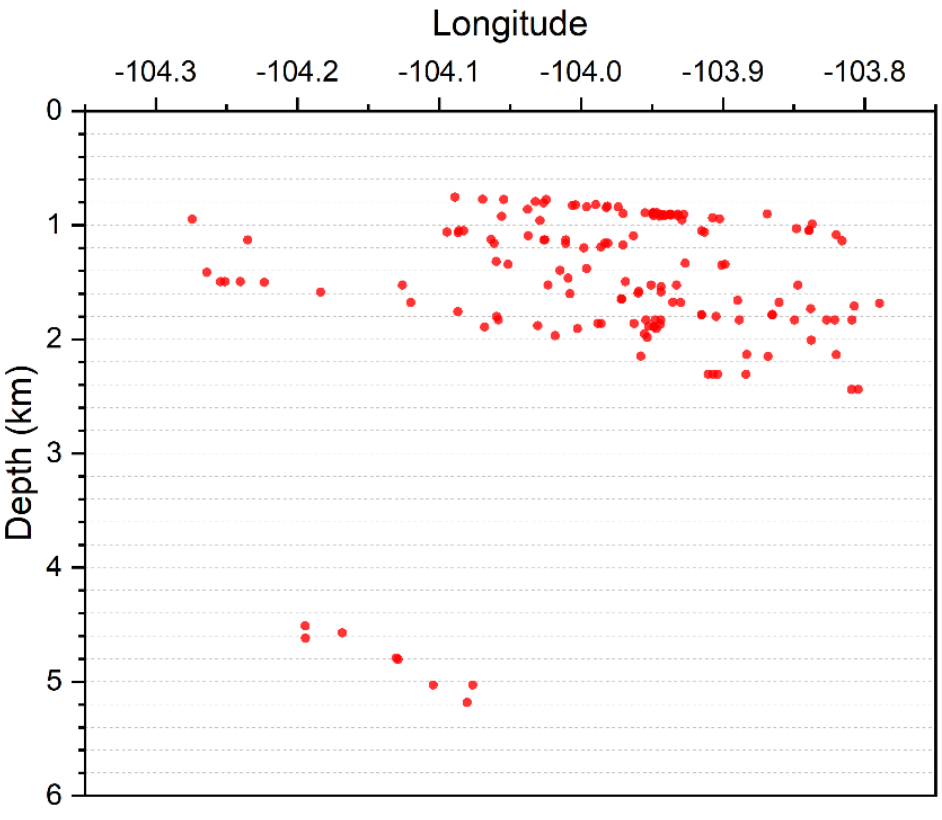

Figure S9. Distribution of well bottom depth.

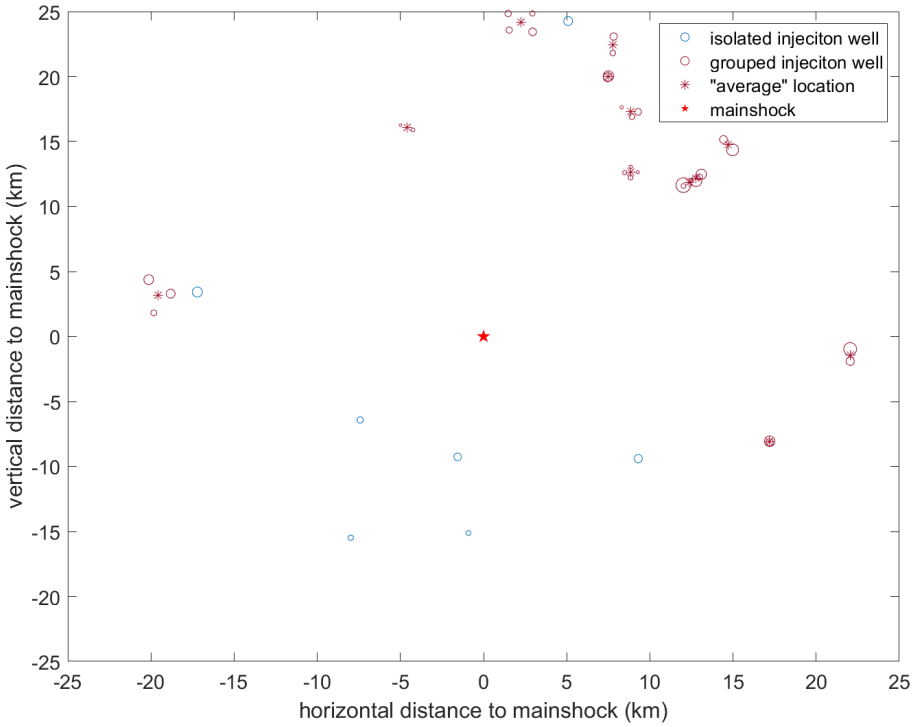

Figure S10. Distribution of injection wells and the averaged location of selected wells. Blue and brown circles represent isolated and grouped injection wells, respectively. The size of the circle is proportional to the total injection volume of injection wells. Brown asterisks indicate the averaged well locations. The red star is the mainshock location.

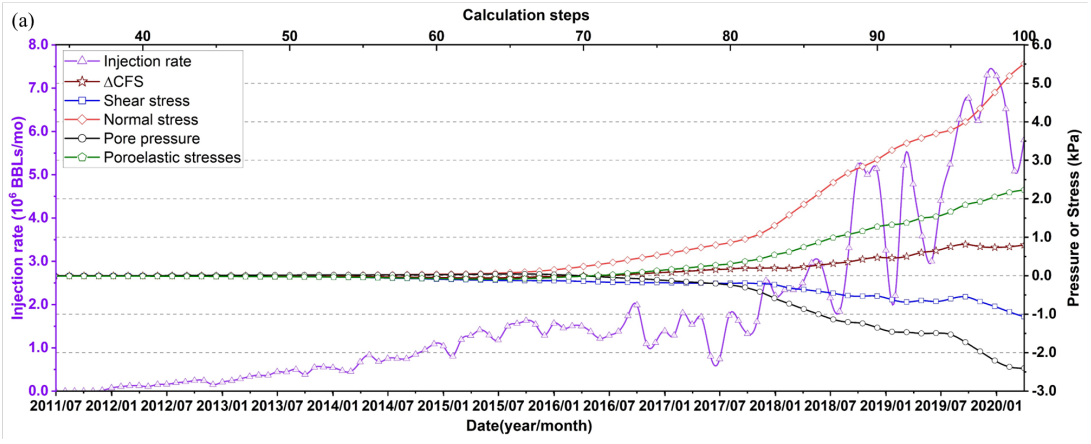
(a)
Calculation steps
Injection rate
ΔCFS
Shear stress
Normal stress
Pore pressure
Poroelastic stresses
Injection rate (10^6 BBLs/mo)
Pressure or Stress (kPa)
Date(year/month)

62

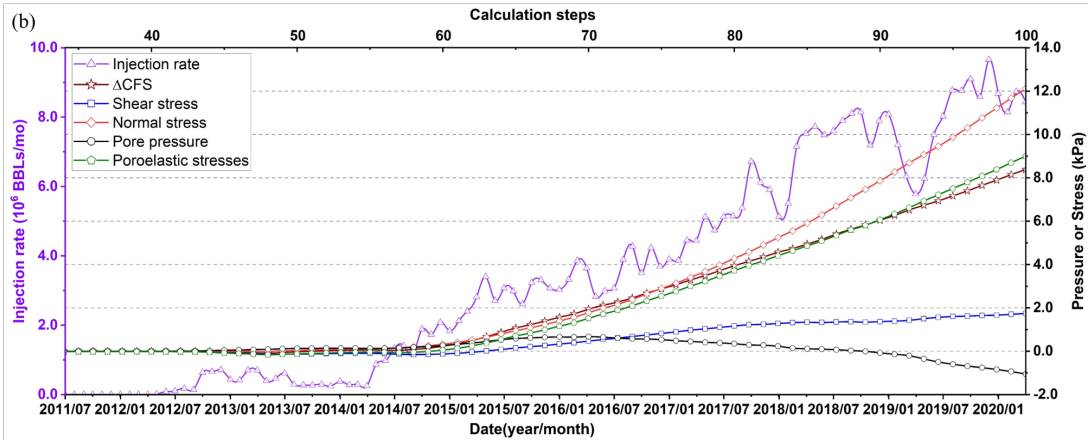
(b)
Calculation steps
Injection rate
ΔCFS
Shear stress
Normal stress
Pore pressure
Poroelastic stresses
Injection rate (10^6 BBLs/mo)
Pressure or Stress (kPa)
Date(year/month)

63

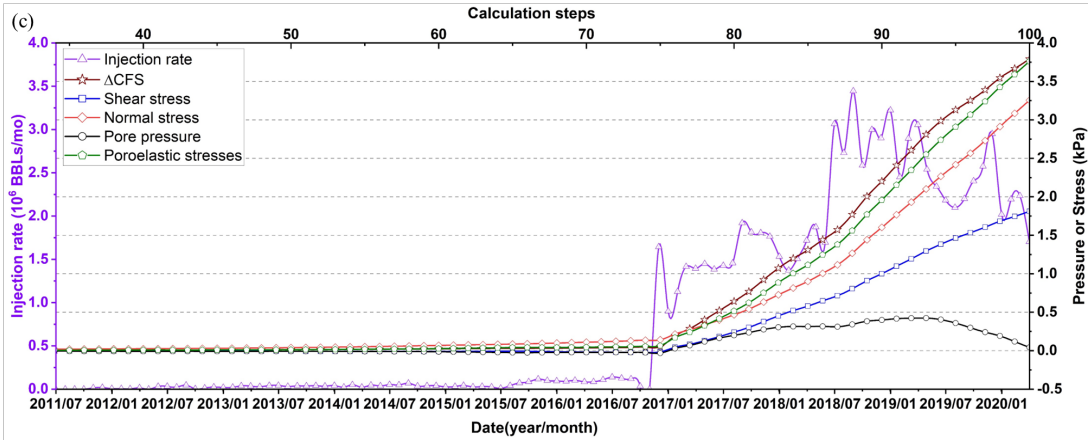
(c)
Calculation steps
Injection rate
ΔCFS
Shear stress
Normal stress
Pore pressure
Poroelastic stresses
Injection rate (10^6 BBLs/mo)
Pressure or Stress (kPa)
Date(year/month)

64

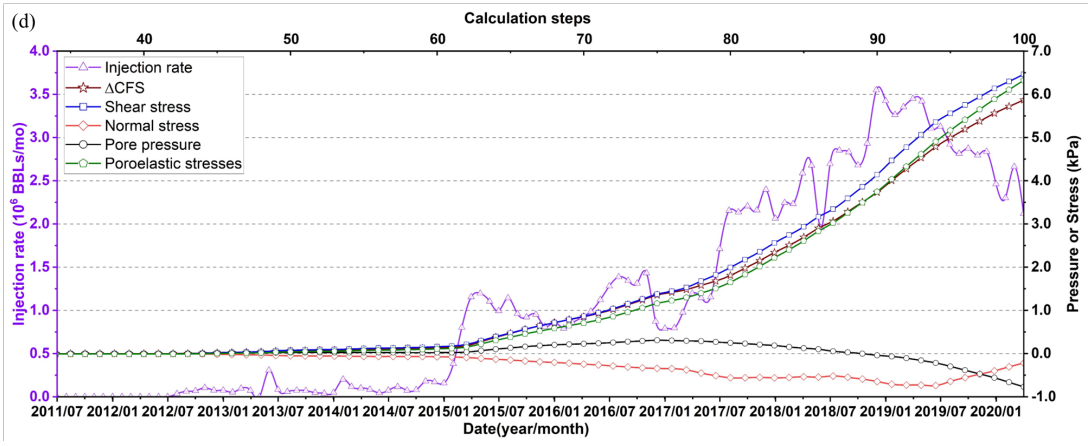

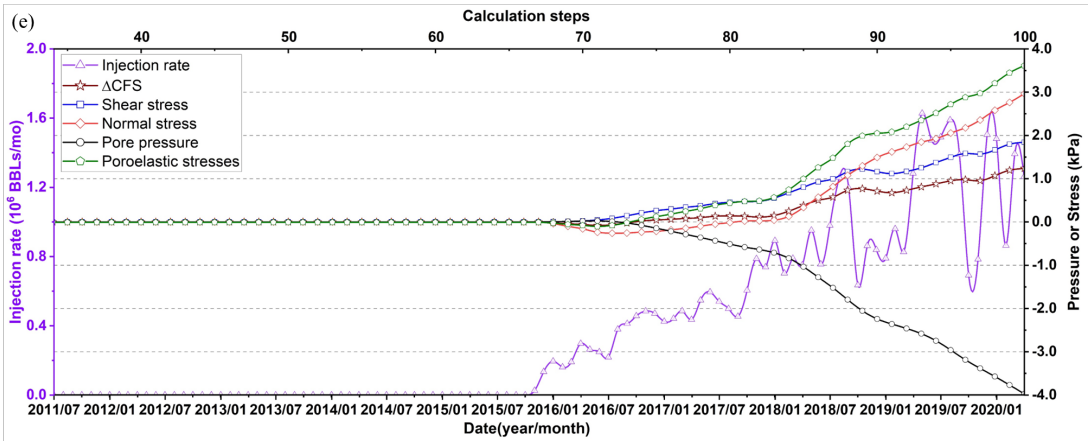

Figure S11. Time evolution of the monthly injection rate of selected deep (a) and shallow (b, c, d, and e corresponds to the northeast, northwest, southeast and southwest quadrants to the M5.0 event) injection wells, as well as the change in pore pressure, poroelastic stress, normal stress, shear stress and ΔCFS on the fitted fault plane near the mainshock location until the occurrence of the M5.0 mainshock.

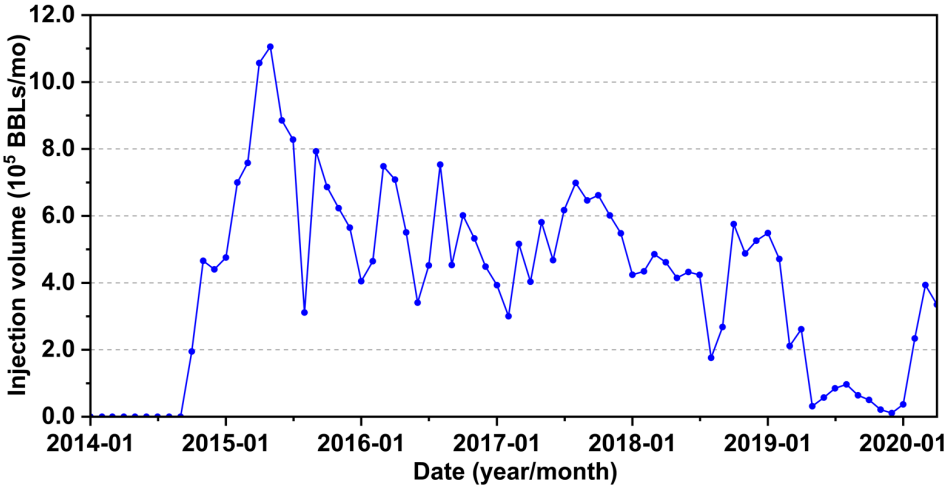

Figure S12. Monthly injection rate of selected shallow injection well (This well has no injection activity prior to January 2014).

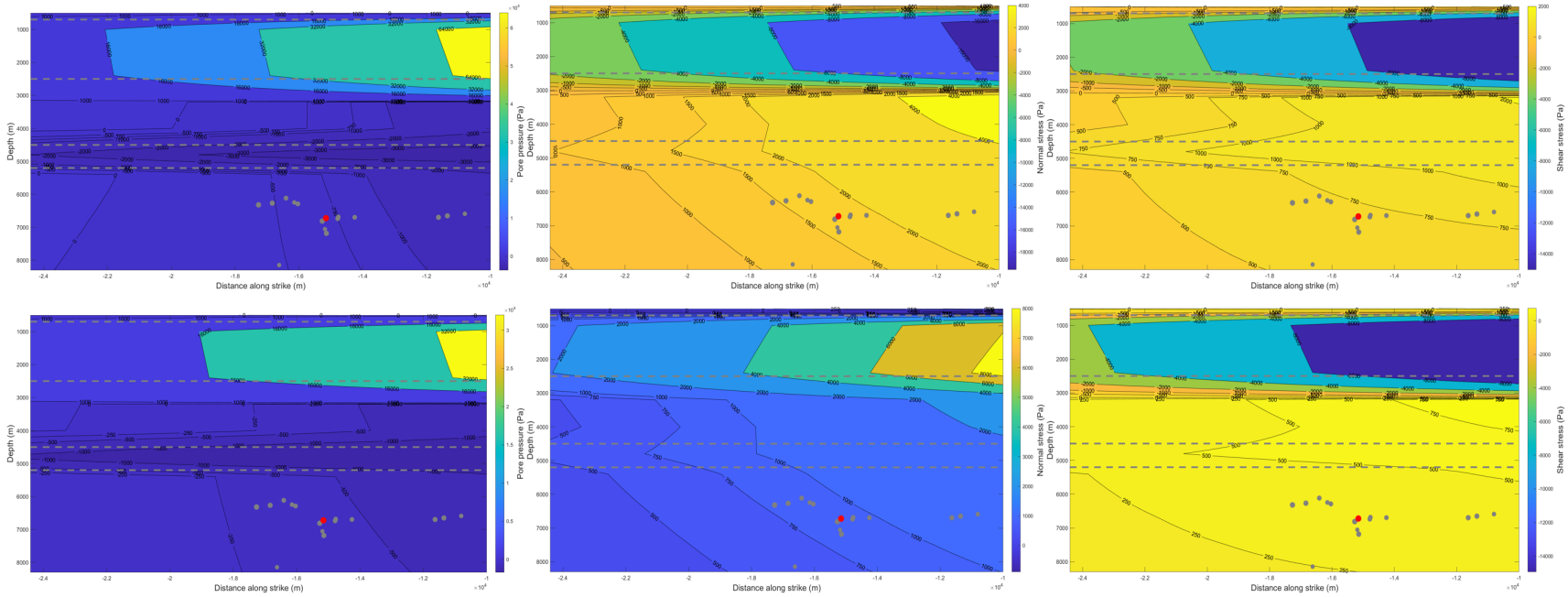

Figure S13. Resulted pore pressure, normal stress and shear stress of injection scenarios SI-1 and SI-2 (Top row: injection scenario SI-1, bottom row: injection scenario SI-2. From left to right: Pore pressure, normal stress, shear stress). Gray dashed lines separate the anhydrite/halite, sandstone, shale, limestone and basement layers (from top to bottom).

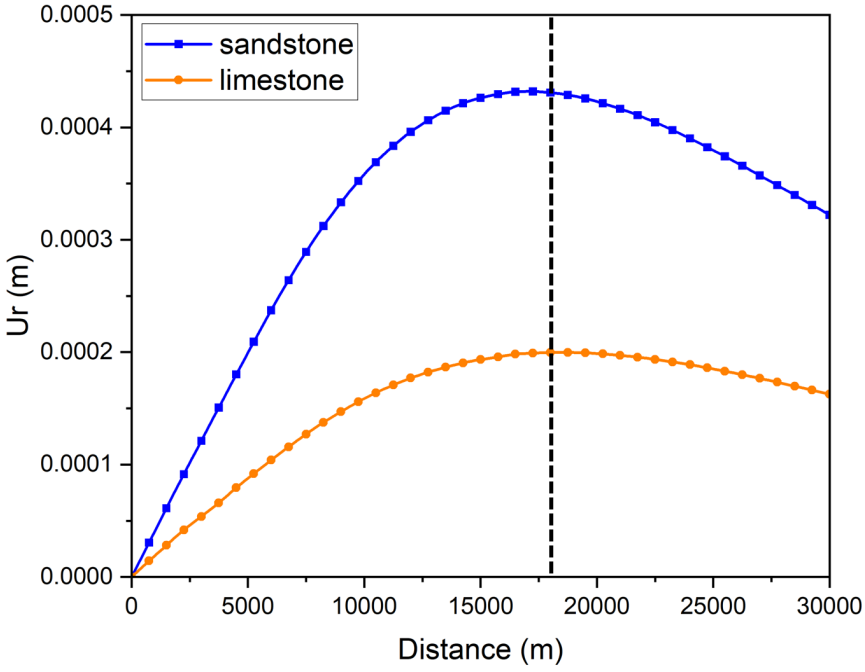

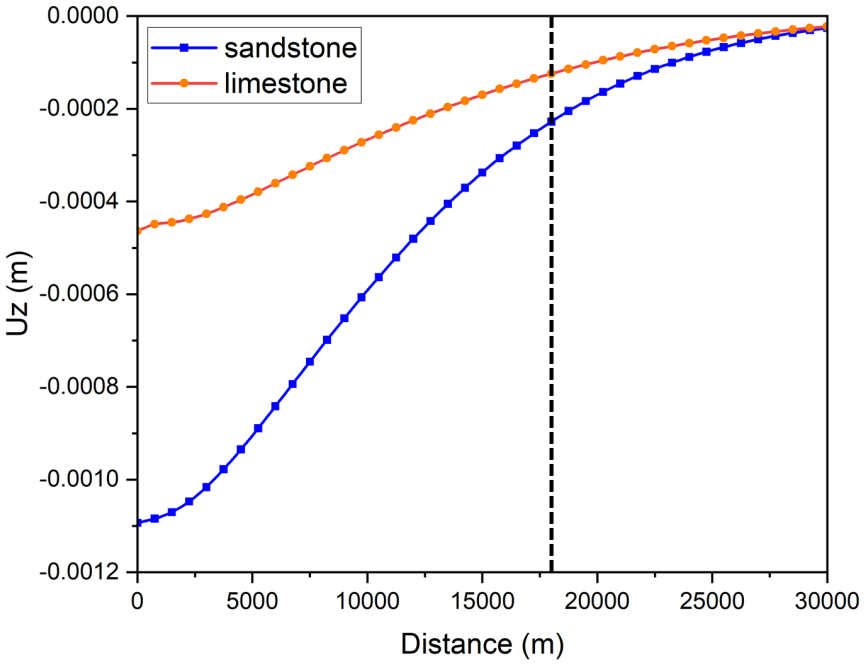

Figure S14. Simulated poroelastic deformation in the r and z direction within the basement layer where the mainshock occurred (depth = 6.7 km) as a result of shallow injections in scenario SI-1 (sandstone layer) and SI-2 (limestone layer), respectively. Here the injection is assumed to occur at distance = 0 m, and the dashed line indicates the mainshock location (a lateral distance of about 18 km from the injection source).

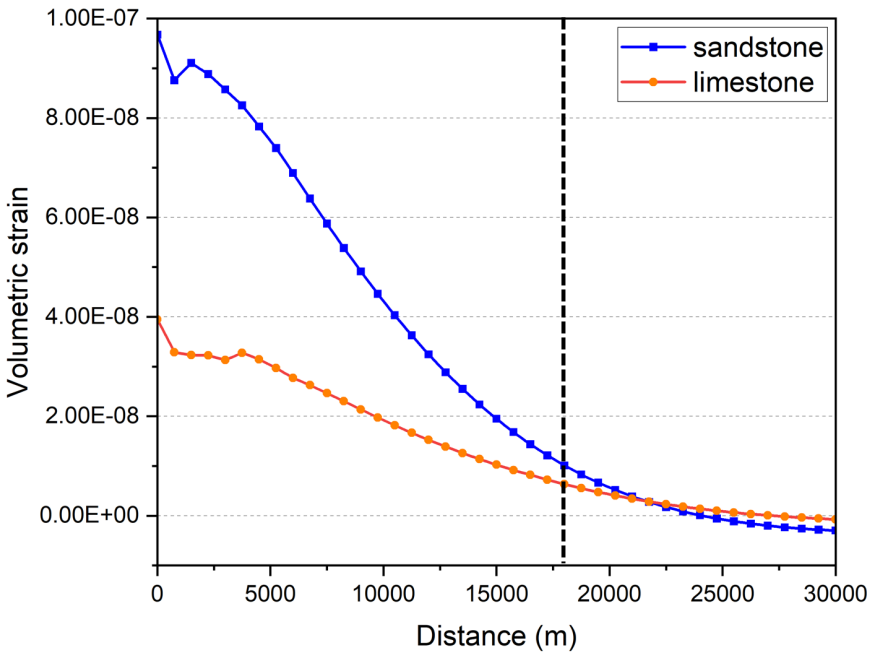

87

88 **Figure S15.** Resulted volumetric strain within the basement layer (at depth of 6.7 km) versus
89 lateral distance from injection source in scenarios SI-1 (sandstone layer) and SI-2 (limestone
90 layer). Here the injection is assumed to occur at distance = 0 m, and the dashed line indicates the
91 mainshock location (a lateral distance of about 18 km from the injection source).

Table S1. Information of seismic stations used in earthquake relocation.

Station name	Latitude	Longitude	Distance to mainshock (km)
TXMB01	31.6677	-102.0829	185.80
TXMB02	31.1981	-102.0379	198.96
TXMB04	32.6254	-102.488	177.85
TXMB05	32.6265	-101.8597	229.20
TXMB06	31.978	-101.8	214.16
TXMB07	32.0006	-102.2528	172.21
TXPB01	30.9437	-103.7811	89.24
TXPB03	31.0838	-103.5139	86.30
TXPB04	31.187	-103.2693	94.04
TXPB05	30.9199	-103.3248	111.65
TXPB06	31.6472	-103.2182	78.48
TXPB07	31.5794	-103.6679	38.61
TXPB08	30.8917	-102.9074	141.54
TXPB09	31.7741	-104.3014	25.40
TXPB10	31.2836	-103.7546	55.25
TXPB11	31.9355	-104.0341	24.26
TXPB12	31.2132	-103.9577	56.41
TXPB13	31.5542	-103.8459	25.90
TXPB14	31.1293	-103.1511	106.85
TXPB15	31.2114	-103.0844	106.87
TXPB16	31.125	-103.252	99.73
TXPB17	30.9968	-103.1518	116.38
TXPB18	31.2008	-103.1996	98.40
TXPB19	31.3031	-103.0997	100.57
TXPB21	31.3419	-103.0622	101.91
TXPB27	31.5763	-103.1307	87.82
TXPB28	31.6686	-104.5008	43.83
TXPB29	31.753	-104.5145	44.96
TXPB30	31.2804	-103.3227	83.72
USMNTX	31.6985	-105.3821	127.06
4TNM01	32.3551	-103.3985	93.29
4TNM02	32.2641	-103.879	62.61
4TNM03	32.4726	-103.6343	92.22

SCPDB	32.0722	-103.5966	57.69
GMNMP01	32.2048	-103.8605	56.76
TXVHRN	30.7866	-104.9852	136.78
TXALPN	30.3745	-103.6385	153.72
SCJAL	32.2024	-103.2293	93.81
GMNMP02	32.0895	-103.8614	44.71
TXPCOS	31.4089	-103.5102	60.94
TXODSA	32.1201	-102.5491	148.10

93

Table S2. Input parameters used in hypoDD. (MINWGHT: minimum pick weight allowed, MAXDIST: maximum distance in km between event pair and stations, MAXSEP: maximum hypocentral separation in km, MAXNGH: maximum number of neighbors per event, MINLINK: minimum number of links required to define a neighbor, MINOBS: minimum number of links per pair saved, MAXOBS: maximum number of links per pair saved, NITER: number of iterations used for listed weights, WTCCP and WTCCS: weight of cross P wave and S wave, WRCC and WRCT: residual threshold in seconds for cross and catalog data, WTCTP and WTCTS: weight of catalog P wave and S wave, WDCC and WDCT: maximum distance (km) between cross and catalog linked pairs, DAMP: damping parameters used in iteration.

MINWGHT	MAXDIST	MAXSEP	MAXNGH	MINLINK	MINOBS	MAXOBS
0	400	6	8	8	1	50

NITER	WTCCP	WTCCS	WRCC	WDCC	WTCTP	WTCTS	WRCT	WDCT	DAMP
5	0.01	0.01	-9	-9	1.0	0.5	-9	-9	40
5	1	0.5	-9	6	0.001	0.001	-9	5	40
5	1	0.5	-9	5	0.001	0.001	6	5	40
5	1	0.5	6	5	0.001	0.001	6	5	40
5	1	0.5	6	3	0.001	0.001	6	3	40

Table S3. Results of jackknife resampling performed on clusters I, II and III and their uncertainty estimations.

fault-I 16 events		fault-II 8 events		fault-III 12 events	
strike	81	strike	95	strike	113
dip	52	dip	58	dip	73
Jackknife sampling 1000 times					
std(strike)	1.01	std(strike)	3.72	std(strike)	10.01
std(strike)/81	1.25%	std(strike)/95	3.91%	std(strike)/113	8.86%
std(dip)	6.41	std(dip)	8.57	std(dip)	18.63
std(dip)/52	12.33%	std(dip)/58	14.77%	std(dip)/73	25.52%
Jackknife sampling 2000 times					
std(strike)	0.99	std(strike)	3.78	std(strike)	9.82
std(strike)/81	1.22%	std(strike)/95	3.98%	std(strike)/113	8.69%
std(dip)	6.34	std(dip)	8.71	std(dip)	18.26
std(dip)/52	12.19%	std(dip)/58	15.02%	std(dip)/73	25.01%
Jackknife sampling 3000 times					
std(strike)	1.06	std(strike)	3.74	std(strike)	9.86
std(strike)/81	1.30%	std(strike)/95	3.94%	std(strike)/113	8.73%
std(dip)	6.74	std(dip)	8.59	std(dip)	18.32
std(dip)/52	12.96%	std(dip)/58	14.81%	std(dip)/73	25.09%

Table S4. Information of selected wells and resulted pore pressure, normal stress, shear stress and ΔCFS from POEL modeling. (Total injection volume is from January 2007 to March 2020).

Calculation groups	API number	Injection depth (m)	Total injection (BBLs)	Pore pressure (Pa)	Normal stress (Pa)	Shear stress (Pa)	ΔCFS (Pa)
NW_1_1	10932849	1499.9	26262354	-242.3	1296.9	679.0	1311.8
NW_1_2	10932848	1493.5	25035604	15.5	856.2	504.4	1027.4
NW_1_2	10933282	1493.5	20785411	224.6	570.8	445.0	922.3
NW_1_2	10933281	1493.5	9331550	157.8	226.6	187.7	418.3
NW_2	10931638	1064.4	4004484	-80.9	201.3	3.0	75.3
NW_2	10931565	1057.7	2063288	-31.1	104.1	-7.2	36.6
SE_1	38934609	2438.4	42808426	67.6	301.0	1760.2	1981.4
SE_1	38935413	2438.4	17916180	159.9	8.8	817.8	919.0
SE_2	38933269	1676.4	29133703	-195.0	-174.6	1470.7	1248.9
SE_2	38936297	1729.7	14006303	189.9	-468.5	905.9	738.8
SE_3	38935362	1582.8	17475621	-991.5	114.9	1509.9	983.9
SW_1	10933058	1828.8	14768626	-2416.7	2107.9	1022.2	836.9
SW_2	10932340	1676.4	10615573	-1257.3	1375.2	605.0	675.8
SW_3	10933071	1524.0	7493206	9.3	-522.2	57.4	-250.4
SW_4	38934925	1341.1	6382062	-307.2	3.4	157.9	-24.4
NE_1_1	38934274	1783.1	56124718	-710.7	2867.3	1319.8	2613.8
NE_1_1	38934372	1783.1	5884046	-136.5	314.1	121.4	227.9
NE_1_1	38933271	1798.3	9924847	-288.0	584.4	212.4	390.3
NE_1_2	38934237	2304.3	30472454	-693.9	1717.8	695.0	1309.3
NE_1_2	38934942	2304.3	27914073	-183.6	1370.6	708.7	1420.8
NE_1_2	38934935	2304.3	3625343	-26.6	182.8	86.8	180.6
NE_2	38934929	2304.3	36359171	153.1	1083.0	418.8	1160.4
NE_2	38935968	1656.9	15547400	254.5	346.4	125.0	485.6
NE_3	38934661	1859.3	29089012	100.2	640.1	-301.2	143.0
NE_3	38935357	1091.2	21147125	219.1	334.6	-316.8	15.4
NE_4	38933299	1127.8	15751034	30.5	213.4	-220.8	-74.5
NE_4	38935108	1158.2	7248901	80.7	16.5	-161.8	-103.5
NE_4	38933620	1127.8	10914961	41.8	118.3	-175.9	-79.8
NE_4	38933298	1127.8	10573269	-30.4	207.3	-97.9	8.2
NE_5	38932872	1828.8	11751801	-175.2	494.4	65.2	256.7

NE_5	38936030	1828.8	8596403	81.6	222.9	-38.0	144.6
NE_5	38936032	1828.8	3146446	77.9	51.7	-66.5	11.3
NE_6	38935886	1578.9	14115239	235.6	32.5	-345.3	-184.5
NE_6	38936478	1592.3	8264986	148.0	-2.0	-234.1	-146.6
NE_7	38935373	1859.3	20599155	231.1	73.7	-427.0	-244.1
NE_8	38932527	1889.2	6148354	-181.2	456.7	135.5	300.8
NE_8	38932506	1884.9	4547952	-113.6	324.9	101.3	228.1
NE_8	38932507	1887.6	3713541	-81.2	261.4	85.0	193.1
NE_8	38932528	1866.3	2602393	-87.3	201.7	59.0	127.7

109

Table S5. Information of injection wells: The averaged locations for various well groups, and true well locations for individual wells. Locations in bold are those used in the POEL model.

Calculation groups	API	Latitude	Longitude	Distance to average location (km)
NE_1_1_Average	N/A	**31.82351494**	**-103.9117379**	
NE_1_1	38934274	31.82183915	-103.9151514	0.37
NE_1_1	38934372	31.82122637	-103.9151443	0.41
NE_1_1	38933271	31.82747931	-103.9049179	0.78
NE_1_2_Average	N/A	**31.82631147**	**-103.9070584**	
NE_1_2	38934237	31.82457177	-103.9069582	0.19
NE_1_2	38934942	31.82931111	-103.9037861	0.45
NE_1_2	38934935	31.82505154	-103.9104309	0.35
NE_2_Average	N/A	**31.84990793**	**-103.8867983**	
NE_2	38934929	31.84629835	-103.8838846	0.49
NE_2	38935968	31.85351751	-103.889712	0.49
NE_3_Average	N/A	**31.89709799**	**-103.9629313**	
NE_3	38934661	31.89749479	-103.9627022	0.05
NE_3	38935357	31.89670119	-103.9631604	0.05
NE_4_Average	N/A	**31.93486384**	**-104.0183942**	
NE_4	38933299	31.92817853	-104.0107952	1.03
NE_4	38935108	31.94095599	-104.0108726	0.98
NE_4	38933620	31.94091722	-104.0262918	1.00
NE_4	38933298	31.92940362	-104.0256171	0.91
NE_5_Average	N/A	**31.87259943**	**-103.9486652**	
NE_5	38932872	31.87263544	-103.9438712	0.45
NE_5	38936030	31.86933526	-103.9477686	0.37
NE_5	38936032	31.87582758	-103.9543557	0.65
NE_6_Average	N/A	**31.91921509**	**-103.9596488**	
NE_6	38935886	31.92495056	-103.9593982	0.64
NE_6	38936478	31.91347962	-103.9598994	0.64
NE_7	38935373	**31.93565646**	**-103.9882531**	
NE_8_Average	N/A	**31.83066298**	**-103.9484245**	
NE_8	38932527	31.82703746	-103.9486369	0.40
NE_8	38932506	31.83053056	-103.9524	0.38
NE_8	38932507	31.83436782	-103.9485536	0.41

NE_8	38932528	31.83071608	-103.9441076	0.41
SW_1	10933058	**31.63327297**	**-104.0583867**	
SW_2	10932340	**31.6589148**	**-104.1202048**	
SW_3	10933071	**31.57716872**	**-104.126143**	
SW_4	38934925	**31.58041141**	**-104.0515104**	
SE_1_Average	N/A	**31.70387054**	**-103.8093091**	
SE_1	38934609	31.70808624	-103.8093091	0.47
SE_1	38935413	31.69965483	-103.8093091	0.47
SE_2_Average	N/A	**31.64368585**	**-103.8604012**	
SE_2	38933269	31.64410095	-103.8604012	0.05
SE_2	38936297	31.64327075	-103.8604012	0.05
SE_3	38935362	**31.632051**	**-103.9437564**	
NW_1_1	10932849	**31.74764785**	**-104.2234287**	
NW_1_2_Average	N/A	**31.74531493**	**-104.2486272**	
NW_1_2	10932848	31.7562617	-104.2543393	1.33
NW_1_2	10933282	31.74651467	-104.2404147	0.79
NW_1_2	10933281	31.73316843	-104.2511275	1.37
NW_2_Average	N/A	**31.86179886**	**-104.0906477**	
NW_2	10931638	31.86013189	-104.0867127	0.42
NW_2	10931565	31.86346583	-104.0945826	0.42

112

Table S6. Information of selected deep injection wells for the calculation. The well 10932704 in the last row, which was used in Tung et al. (2021), was not selected due to the long distance from the M5.0 event (~34 km). Instead, we chose the well 10933393 for the calculation. Nevertheless, ΔCFS caused by these two wells are relatively small: For 10932704, ΔCFS = 0.09 kPa, contributing to only 0.1% of the total ΔCFS in Tung et al. (2021); For 10933393, ΔCFS = -11 Pa in our calculation, indicating slip inhibition.

API	Injection depth (m)	Distance (km)	Latitude	Longitude	Total injection volume (BBLS)	ΔCFS (Pa)
10932395	4620	25.3	31.90386751	-104.1944243	30968068	95.26
10932532	4572	29.2	31.95741941	-104.1684945	31391720	-8.06
10932782	4510	18.1	31.81591015	-104.1945797	31218221	467.93
10932982	4804	11.3	31.78707537	-104.1291484	32822464	702.53
10933026	5030	16.7	31.86462427	-104.0764656	16452828	-87.35
10933166	5030	26.2	31.94728703	-104.1043423	19579260	-200.36
10933296	5180	20.9	31.9023804	-104.0804595	14439942	-159.57
10933393	4790	17.8	31.85911977	-104.13036601	4775928	-11.31
10932704	4420	34.1	31.94214235	-104.287393	6589535	

Table S7. Selected shallow injection wells for the sensitivity test. The pore pressure, normal stress, shear stress and ΔCFS listed here are simulation results based on geological model in Table 3.

Calculation groups	API number	Injection depth (m)	Pore pressure (Pa)	Normal stress (Pa)	Shear stress (Pa)	ΔCFS (Pa)
NW_1_1	10932849	1499.9	-242.3	1296.9	679.0	1311.8
NW_1_2	10932848	1493.5	15.5	856.2	504.4	1027.4
SE_1	38934609	2438.4	67.6	301.0	1760.2	1981.4
SE_2	38933269	1676.4	-195.0	-174.6	1470.7	1248.9
SW_1	10933058	1828.8	-2416.7	2107.9	1022.2	836.9
SW_2	10932340	1676.4	-1257.3	1375.2	605.0	675.8
NE_1_1	38934274	1783.1	-710.7	2867.3	1319.8	2613.8
NE_1_2	38934237	2304.3	-693.9	1717.8	695.0	1309.3
NE_1_2	38934942	2304.3	-183.6	1370.6	708.7	1420.8
NE_2	38934929	2304.3	153.1	1083.0	418.8	1160.4

Table S8. Results of sensitivity test. The pore pressure, shear and normal stresses, and total ΔCFS shown are the cumulative values from 10 shallow injection wells.

Parameters changed compared to geological model in Table 3	Total pore pressure (Pa)	Total normal stress (Pa)	Total shear stress (Pa)	Total ΔCFS (Pa)
Shale layer: ν_u = 0.47, B=0.94 (identical to the model in Tung et al. (2021))	-5479.74	12703.49	9134.75	13469.00
Shale layer: B=0.7	-5436.27	12754.56	9170.12	13561.10
Shale layer: B=0.8	-5412.86	12706.84	9156.83	13533.22
Shale layer: B=0.9	-5384.33	12663.07	9142.37	13509.61
Sandstone layer: D=0.1	3365.62	6624.91	11489.57	17483.89
Sandstone layer: D=0.5	-4339.12	12197.14	9757.51	14472.33
Sandstone layer: D=1.0	-6727.20	13097.33	8056.28	11878.36

Table S9. Seismic activity within 10 km of the mainshock ranges from 2017 to 2021 from the TexNet earthquake catalog.

Table S10. Information of selected shallow injection well (SI-1).

API	UIC number	Injection depth (m)	Latitude	Longitude	Total injection volume (BBLS)
38934237	000108878	2305	31.825	-103.90695815	30472454

Video S1. Temporal and spatial evolution of seismic activities within 10 km of the M5.0 Mentone earthquake from 2017 to 2021.

References

Sheng, Y., Pepin, K. S., & Ellsworth, W. L. (2022). On the depth of earthquakes in the Delaware Basin: A case study along the Reeves–Pecos county line, *Seismol. Rec.* **2,** no. 1, 29–37.

Tung, S., Zhai, G., & Shirzaei, M. (2021). Potential link between 2020 Mentone, West Texas M5 earthquake and nearby wastewater injection: implications for aquifer mechanical properties, *Geophys. Res. Lett.* **48,** no. 3, doi: 10.1029/2020GL090551.